The performance of High-Index-Contrast Photonics Platforms for On-Chip Raman Spectroscopy

A. Raza,[1,2*] S. Clemmen,[1,2] M. de Goede,[3] R. Ali,[4] P. Hua,[5] S. M. Garcia-Blanco,[3] S. Honkanen,[4] J. S. Wilkinson, [5] and R. Baets[1,2]

[1]Photonics Research Group, INTEC Department, Ghent University-imec, Technologiepark—Zwijnaarde, 9052 Ghent, Belgium
[2]Center of Nano and Biophotonics, Ghent University, Belgium
[3]Optical Sciences Group, MESA+ Institute of Nanotechnology, University of Twente, 4617, The Netherlands
[4]Institute of Photonics, University of Eastern Finland, 80101, Finland
[5]Optoelectronics Research Centre (ORC), University of Southampton, Highfield, Southampton, SO17 1BJ, United Kingdom
**Corresponding author: ali.raza@ugent.be*

Various photonic platforms exist that may be suitable for on-chip Raman spectroscopy. Here we compare 4 of them focusing on their intrinsic photon background and their capability for collecting Raman signal from liquid analytes. These two parameters define the complete figure of merit for waveguide enhanced Raman spectroscopy.

Keywords: Raman spectroscopy, Waveguide enhanced Raman sensing, HIC waveguides

Enhancing the light mater interaction is highly desirable for Raman spectroscopy because of the fundamentally weak Raman scattering cross sections. Hollow optical fibers and more recently nanophotonic waveguides have exhibited enhancement in Raman signal by many orders of magnitude over traditional Raman microscope [1, 2]. Rib waveguides can be used as easily as cover slides and have therefore been used for Raman spectroscopy of various analytes such as bulk liquids [3-5], adsorbed monolayers [6] as well as in gaseous state [7]. Many photonics platforms exist that may seem suitable for a Raman spectroscopy sensor, but a good waveguide-based Raman sensor requires qualities that may contradict each other. The waveguide need to be low loss to maximize the effective interaction length. At the same time, it needs to have a large index to be able to push a significant part of the field into the analyte out of the waveguide while still keeping good guiding properties. The waveguide must also handle large optical power. Finally, it should not induce any photon background that may overlap spectrally with the Raman signal. All these properties impact directly on the signal to noise ratio and may relax strongly the otherwise tight specifications required for light sources and photodetectors of a Raman spectroscopy system. In this report, we compare 4 photonic platforms and present measurements of their broadband photon background. The four platforms under investigation are PECVD Si_3N_4, ALD grown TiO_2, sputtered Ta_2O_5 and reactive co-sputtered Al_2O_3. To measure the Raman background of these waveguide materials, strip waveguides were fabricated on top of a silica substrate using traditional fabrication techniques e.g. Al_2O_3, Si_3N_4 and Ta_2O_5 waveguides were fabricated using deep UV lithography while ALD grown TiO_2 were patterned using e-beam lithography. The fabrication details of each waveguide can be found in [8-11]. The fabricated waveguide geometries, refractive indices and corresponding waveguide losses are presented in Table 1. It is worth noting that those geometries are not optimized for a use in Raman spectroscopy that typically requires smaller dimensions so that the field couples evanescently to an analyte. Therefore, scattering loss for an optimized waveguide may be underestimated. The total backscattered background P_s normalized by total guided power P_0 can be estimated by assuming it has a Raman origin. In a waveguide of length *L*, width *w* and height *h* and propagation loss α can be computed using

$$\frac{P_s}{P_0} = \frac{1}{2} \times \rho\sigma\eta_{BG}\,\gamma^2 \times \left(\frac{e^{-2\alpha L} - 1}{2\alpha}\right)$$

where ρ and σ are respectively the molecular density and Raman cross section of the waveguide material, γ is the coupling efficiency. η_{BG} is background conversion efficiency that quantifies the amount of a background signal collected in a waveguide mode. The values of η_{BG} depends on the geometry and the index contrast of the waveguide. Using COMSOL Multiphysics mode solver, we deduced η_{BG} for the 4 waveguides assuming 785 nm pump wavelength and 820 cm^{-1} stokes shift (Table 1).

The background spectra are measured from the 4 waveguides using a confocal setup [12]. A 785 nm pump is used to excite the TE fundamental mode in a waveguide using high NA 0.9/100× objective. The backscattered signal is collected using the same objective and the Raman Stokes scattered signal is sent to -73°C cooled Andor

IDUS 401 CCD camera after the remaining pump is rejected by a spectral filter. Furthermore, an integrating sphere at the output side of the waveguide is used to measure the transmission and the coupling efficiency.

Waveguide	Cross section (width (nm) × (nm) height)	Refractive index	Waveguide loss (dB/cm)	η_{BG}
Al_2O_3	2400 × 550	1.64	2.2	0.2114
Si_3N_4	700 × 220	1.90	4.3	0.5405
Ta_2O_5	1000 × 550	2.11	4.0	0.6321
TiO_2	1000 × 450	2.36	8.2	0.6901

Table 1.The optical properties of different photonics plat forms under discussion.

The measured Raman spectra σ* are plotted in Fig. 1 and are normalized by ɣ, η_{BG} and length factor. The error bar in Fig 1. represents the deviation of signal over five different waveguide on same chip. TiO_2 exhibits a large Raman background that is an order of magnitude stronger as compared to other three materials. The other three waveguide materials are in close competition and outperform each other depending on the Raman frequency under interest. Therefore, Al_2O_3 may suffer from low collection efficiency from an analyte lying uniformly over the waveguide length. However, Si_3N_4 and Ta_2O_5 seem to have similar performance in term of the Raman background.

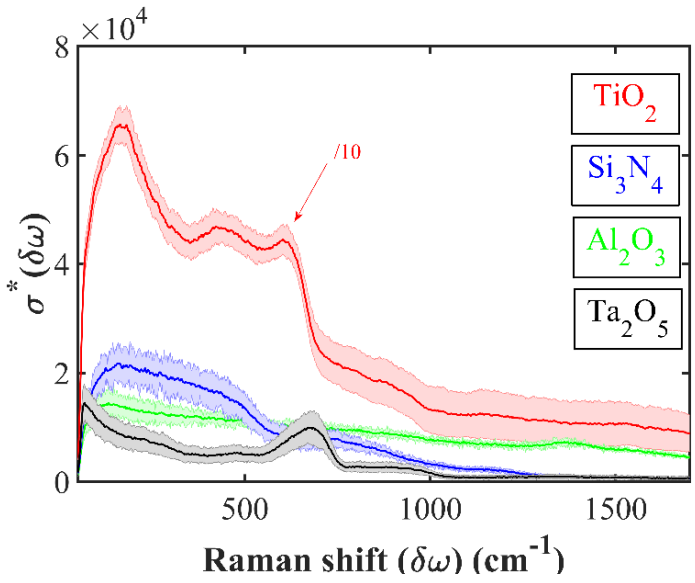

Figure 1. The normalized Raman background of four photonics platform. . The TiO_2 Raman spectrum is normalized by 10 for visual guidance.

In the latter part, we have computed the analyte signal collection efficiency $\eta_{Analyte}$ [2] for all the four photonics platforms. For this purpose, we assume a uniform covering of the waveguides with an analyte having refractive index 1.37 and a Raman mode around 819 cm^{-1} i.e. isopropanol [2]. The Raman collection efficiency $\eta_{Analyte}$ for each is material is maximized by adjusting the geometry of the waveguide assuming the same pump wavelength of 785 nm and 819 cm^{-1} Raman shift. The results of these simulations are summarized in Table 2. Owing to high index contrast, TiO_2 waveguide leads to the high collection efficiency while the Al_2O_3 waveguide suffers due to low index contrast. On the other hand Si_3N_4, and Ta_2O_5 offers similar magnitude of collection efficiency.

Waveguide	Cross section (width (nm) × height (nm))	$\eta_{Analyte}$
Al_2O_3	325 × 1200	0.0395
Si_3N_4	200 × 550	0.1721
Ta_2O_5	175 × 425	0.2667
TiO_2	150 × 375	0.3745

Table 2.The signal collection efficiency $\eta_{Analyte}$ from an analyte lying uniformly on a waveguide.

As a conclusion, we have presented the performance of four different high index contrast photonic platforms in term of photon background and signal collection efficiency. TiO_2 has the higher collection efficiency but its performance suffers due to huge photon background. On the other hand, Al_2O_3, Si_3N_4 and Ta_2O_5 have same photon

background that is an order of magnitude less than TiO_2. Si_3N_4 and Ta_2O_5 looks equally promising as their photon background is low and similar high index contrasts leads to high signal collection efficiency.

Acknowledgement

The authors acknowledge Prof. N. Le Thomas and Dr. Pieter Wuytens for useful feedback. The authors would like to thank the FWO and ERC-InSpectra for their financial support.

REFERENCES

[1] S. O. Konorov, et al. "Hollow-core photonics crystal fiber-optic probes for Raman spectroscopy," Opt. Lett. 31(12), 1911-1913, (2006).

[2] A. Dhakal, et al. "Efficiency of evanescent excitation and collection of spontaneous Raman scattering near high index contrast channel waveguides," Optics Express 23(21), pp.27391-27404 (2014).

[3] A. Dhakal, et al. "Evanescent excitation and collection of spontaneous Raman spectra using silicon nitride nanophotonic waveguides," Opt. Lett. 39(13), pp.4025-4028 (2014).

[4] C. C. Evans, et al. "TiO_2 Nanophotonic Sensors for Efficient Integrated Evanescent Raman Spectroscopy," ACS Photonics 3(9), pp.1662 (2016).

[5] Z. WANG, et al. "Surface and waveguide collection of Raman emission in waveguide-enhanced Raman spectroscopy," Opt. Lett. 41(17), 4146-4149 (2016).

[6] A. Dhakal, et al. "Nanophotonics waveguide enhanced Raman spectroscopy of biological sub monolayers," ACS Photonics 3(11), 2141 (2016).

[7] S. A. Holmstrom, et al. "Trace gas Raman spectroscopy using functionalized waveguides," Optica 3(8), 891-896 (2016).

[8] A. Subramanian, et al. "Low-Loss Single mode PECVD silicon nitride photonic wire waveguides for 532-900 nm wavelength window fabricated within a CMOS pilot line," IEEE Photonics Journal 5(6), 2202809 (2013).

[9] B. S. Ahluwalia, et al. "Fabrication of Submicrometer High Refractive Index Tantalum Pentoxide Waveguides for Optical Propulsion of Microparticles," IEEE Phot. Tech. Lett. 21, 1408 (2009).

[10] M. Hayrinen, et al. "Titanium dioxide slot waveguides for visible wavelengths," Applied Optics 12, 2653-2657 (2015).

[11] J. D. B. Bradley, et al. "Fabrication of low-loss channel waveguides in Al_2O_3 and Y_2O_3 layers by inductively coupled plasma reactive ion etchng," Appl. Phys. B 89, 311-318 (2007).

[12] P. Wuytens, et al. "On-chip surface-enhanced Raman spectroscopy using Nano sphere-lithography patterned antennas on silicon nitride waveguides". Optics Express, 25(11), 12926–12934 (2017).